Macromolecules

ARTICLE

pubs.acs.org/Macromolecules

Probing the Scope of Crystallization-Driven Living Self-Assembly: Studies of Diblock Copolymer Micelles with a Polyisoprene Corona and a Crystalline Poly(ferrocenyldiethylsilane) Core-Forming Metalloblock

Torben Gädt,[†] Felix H. Schacher,[†,§] Nina McGrath,[†] Mitchell A. Winnik,[*,‡] and Ian Manners[*,†]

[†]School of Chemistry, University of Bristol, Bristol BS8 1TS, U.K.

[‡]Department of Chemistry, University of Toronto, Toronto, ON, Canada M5S 3H6

Supporting Information

ABSTRACT: Diblock copolymers with a crystalline poly(ferrocenyldimethylsilane) (PFDMS) core-forming block have been previously shown to self-assemble in selective solvents for a coblock such as polyisoprene (PI) to form cylindrical micelles (where the material is asymmetric, with a PI:PFDMS block ratio of ca. >5:1) or platelets (where the block ratio is ca. 1:1). Moreover, upon addition of further cylinder-forming block copolymer to the ends of the crystalline cores of the cylinders, the faces of the platelets and also the surfaces of thin films of PFDMS homopolymer has been shown to initiate the further growth of cylinders by a living self-assembly process. This is believed to involve an epitaxial growth mechanism. To obtain more detailed insight and to examine the generality of this behavior, we report here detailed comparative studies of the analogous poly(ferrocenyldiethylsilane) (PFDES) homopolymer and the corresponding PI−PFDES diblock copolymers. Significantly, although PI-*b*-PFDES diblock copolymers with a semicrystalline PFDES core-forming block show similarities to their known PFDMS counterparts in terms of their self-assembly behavior in selective solvents for PI, important differences were also observed. For example, a pronounced tendency of PFDES diblock copolymers to form tape-like structures in solution was noted for PI:PFDES block ratios of ca. 6:1. Uniform cylindrical structures were obtained as the exclusive morphology by increasing the length of the PI block to block ratios of 19:1. Nevertheless, the successful crystallization-driven living self-assembly of PFDES block copolymers involving homoepitaxial growth was demonstrated by the addition of block copolymer unimers to preformed stub-like crystallites formed by sonication. This allowed controlled growth of monodisperse cylinders with the length controlled by the unimer to seed ratio. However, heteroepitaxial growth of PFDES block copolymer from seed micelles of the PFDMS analogue (and vice versa) could not be accomplished. This may be a consequence of the lattice mismatch between the materials and/or kinetic effects. The results demonstrate that crystallization-driven living self-assembly is not limited to PFDMS diblock copolymers and suggest that, although significant differences in self-assembly behavior are likely, this process may be expected to be applicable to other diblock copolymers with a semicrystalline core-forming block.

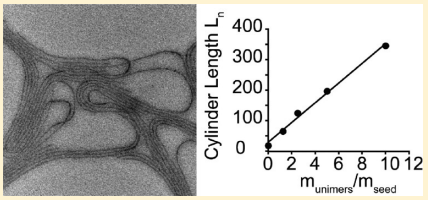

INTRODUCTION

The controlled bottom-up fabrication of nanomaterials with well-defined but complex architectures represents a synthetic challenge of widespread current interest. The solution self-assembly of amphiphilic coil−coil block copolymers with immiscible blocks in block-selective solvents is a promising strategy for the preparation of these materials and has been well-studied where both blocks are amorphous. A variety of different morphologies such as spheres, cylinders, and vesicles has been realized. These structures have potential applications in areas as diverse as drug delivery and nanolithography.[1] By changing the block ratio, the solvent selectivity, or the temperature, transitions between these morphologies can be induced.[2] Very recently, complex structures such as striped cylinders, toroids, and multicompartmental micelles have been also been prepared by self-assembly processes.[3]

The solution self-assembly of crystalline−coil block copolymers provides a promising approach to nanomaterials where the formation of nanoscale aggregates is influenced by the crystallization of a block copolymer in solution. The first solution self-assembly studies of coil−crystalline diblock copolymers with a crystalline core-forming block were reported by Lotz and Keller in 1966. These workers studied the crystallization of poly(ethylene oxide)-*block*-polystyrene (PEO-*b*-PS) in a selective solvent for PS and described the formation of square platelets with a crystalline PEO core.[4] In fact, until recently, crystalline−coil diblock copolymers were generally found to self-assemble into platelet-like structures in a selective solvent for the amorphous block.[5,6]

Polyferrocenylsilane (PFS) block copolymers are an interesting class of new materials with a range of properties and functions

Received: December 22, 2010
Revised: March 26, 2011
Published: April 22, 2011

that complement those available from their all-organic analogues as a result of the presence of metal centers.[7] For example, the redox activity of the PFS block leads to the formation of semiconductive phase-separated nanodomains in the solid state, and the redox reversibility has been used to influence phase-separated morphologies in thin films and to control micelle formation in solution.[8] The presence of relatively electron-rich elements Fe and Si in a PFS block allows intrinsic nanodomain contrast and elemental mapping opportunities in TEM experiments and provides, for example, key advantages for the exploration of the phase separation of block copolymers in confined geometries.[9] Recent work has also taken advantage of the plasma etch resistance of PFS blocks to fabricate nanostructured surfaces for magnetic data storage and SERS applications.[10] The ability of the PFS block to convert thermally into ceramic nanodomain replicas containing Fe nanoparticles that are magnetic and catalytically active has also been investigated and exploited in device fabrication.[11]

We have previously shown that asymmetric diblock copolymers with a much shorter crystalline core-forming poly(ferrocenyldimethylsilane) (PFDMS, see Chart 1) metalloblock yield well-defined cylindrical micelles in a selective solvent for the longer complementary coblock, such as polyisoprene (PI).[12] The crystallization of the PFDMS core apparently directs the self-assembly of PI-*b*-PFDMS and related materials toward a structure with lower interfacial curvature compared to that present in spherical star-like micelles, the expected, and in several cases demonstrated morphology for all-amorphous PFS block copolymer analogues.[12a] More recently, we have found that the termini of the cylindrical micelles remain active to the addition of further PFS block copolymer unimers.[13] This novel growth process is apparently driven by epitaxial crystallization of the core-forming PFS block (Scheme 1, left). Epitaxial growth processes have already been studied in thin films and bulk samples of crystalline−coil block copolymers.[14] In our case, using very small seed micelles present in solution, well-defined and monodisperse cylindrical micelles can be created with lengths dependent on the seed-to-unimer ratio. This can be regarded as a living self-assembly process by analogy with classical living covalent polymerizations.[15] In addition, we have shown that epitaxial growth of cylindrical PFDMS block copolymer micelles can be achieved from the edges of platelet micelles and even from the surface of thin films of PFDMS homopolymer.[16] Furthermore, addition of a PFDMS block copolymer with a different corona-forming block to preexisting cylinders allows the formation of block comicelle architectures (Scheme 1, right). Heteroepitaxial growth has also been demonstrated and the addition of analogous poly(ferrocenyldimethylgermane) (PFDMG) block copolymers to cylinders formed from PFDMS analogue yields block comicelles with a segmented core and PFDMS−PFDMG heterojunctions.[16] The new synthetic method may also be transferable to other crystalline−coil block copolymer systems, including those involving π-conjugated blocks. Thus, the ability of crystallization-driven living self-assembly to allow versatile access to multiblock and other hierarchical architectures involving core−core heterojunctions or spatially selective coronal functionalization (e.g., by nanoparticles or metal oxides)[17] suggests intriguing future possibilities for device fabrication and other applications.

A range of other studies since 2000 have also provided ample evidence that the solution self-assembly of crystalline−coil block copolymers represents a very fertile area of future research.[18] For example, elongated micelles have been formed via the cocrystallization of enantiomeric poly(L-lactide)−poly(ε-caprolactone) and poly(D-lactide)−poly(ε-caprolactone) in selective solvents for the poly(ε-caprolactone) block.[18a] Crystallization of the PEO core of poly(ethylene oxide)-*block*-polybutadiene in *n*-heptane has been reported to yield meander-[18d] or rod-like micelles.[18e] The formation of cylindrical or worm-like micelles from diblock copolymers with a semicrystalline block has been reported for diblock copolymers with a polyacrylonitrile core such as polyacrylonitrile-*block*-polystyrene and polyacrylonitrile-*block*-poly(methyl methacrylate) in nonpolar solvents.[18f] Depending on the block ratio and solution temperature, poly(ε-caprolactone)-*block*-poly(ethylene oxide) (PCL-*b*-PEO) forms spheres, cylindrical micelles, or platelets with a crystalline poly(ε-caprolactone) core in aqueous solution.[18g,h] In addition, the thermoreversible formation of worm-like micelles with a crystalline polyethylene core has been demonstrated upon dissolution of a polystyrene-*block*-polyethylene-*block*-poly(methyl methacrylate) (PS-*b*-PE-*b*-PMMA) triblock terpolymer in toluene, acetone, or THF.[18i]

Chart 1. Structures of PFDMS, PFDMG, and PI-*b*-PFDMS Diblock Copolymers

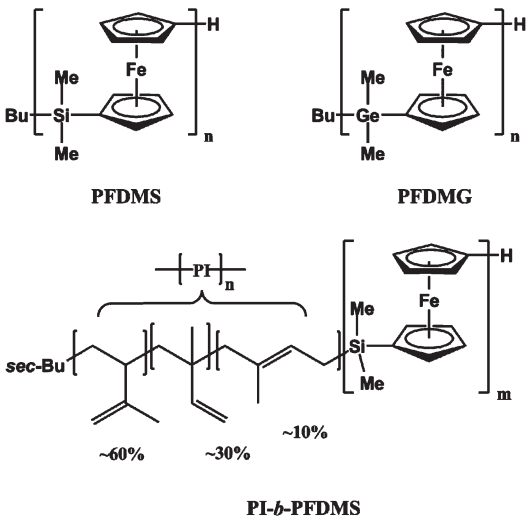

Scheme 1. Epitaxial Growth of Block Copolymer Unimers from Seed Micelles

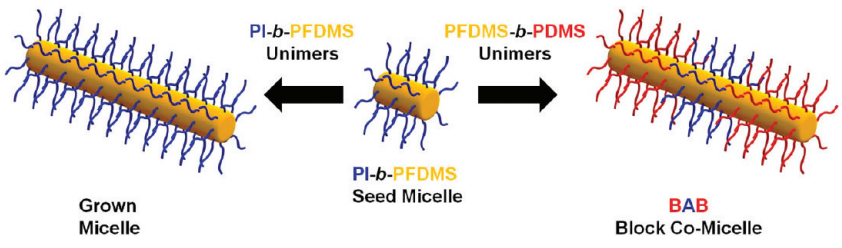

dx.doi.org/10.1021/ma1029289 |*Macromolecules* 2011, 44, 3777–3786

Chart 2. Structures of PFDES and PI-*b*-PFDES Diblock Copolymers

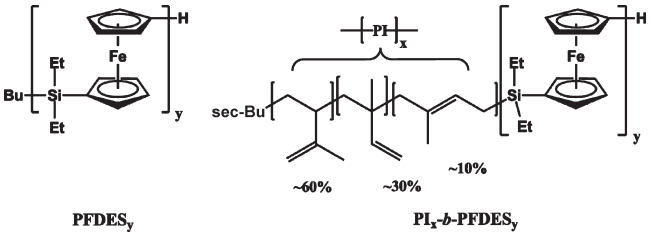

Table 1. Data for PFDES Homopolymers

	M_n(calc)	M_n(obs) GPC	M_n(obs) NMR	PDI
$PFDES_{32}$	7 500	8 600	7 600	1.04
$PFDES_{53}$	15 000	14 300	12 500	1.06
$PFDES_{130}$	30 000	35 000	29 200	1.07

In order to obtain improved understanding and an appreciation of the scope of crystallization-driven living self-assembly processes, further detailed studies of crystalline−coil block copolymers with controlled variations in structure are needed. In this paper we report studies of poly(ferrocenyldiethylsilane) (PFDES) diblock copolymers that are analogous to previously studied PFDMS materials. Our results reveal interesting and significant differences in self-assembly behavior as well as similarities and provide insight into the ability to transpose the crystallization-driven living self-assembly method to a variety of other block copolymers with semicrystalline core-forming segments.

RESULTS AND DISCUSSION

1. Synthesis and Characterization of PFDES Homopolymers and Block Copolymers. Symmetrically substituted poly(ferrocenyldialkylsilane) homopolymers (alkyl = Me, Et, *n*-propyl, *n*-butyl, and *n*-pentyl) are semicrystalline polymers.[19] However, other than the case of PFDMS, none of these materials have been studied in detail, and no block copolymers have been prepared and investigated. Previously, the only reported sample of PFDES homopolymer had been obtained by thermal ring-opening polymerization of the silicon-bridged [1]ferrocenophane [Fe{(η^5-C_5H_4)$_2$SiEt$_2$}] (**1**) and had a molecular weight of M_n = 4.8 × 10^5 g/mol with M_w/M_n = 1.6.[20] We prepared PFDES homopolymers with a narrow weight distribution by living anionic polymerization of **1** using *n*-BuLi as initiator (see Supporting Information and Chart 2). The progress of the polymerization reaction can be conveniently monitored visually since completion of the polymerization is indicated by a color change of the solution from dark red to amber. The anionic polymerization of PFDMS in THF at room temperature goes to completion within ∼10 min for polymers with 50 repeat units (i.e., M_n = 1.2 × 10^4 g/mol).[21] In contrast, the formation of PFDES is considerably slower, and an amber color indicating full conversion is obtained after 4 h. Apart from that difference to its dimethyl analogue, the anionic polymerization of monomer **1** gives polymers with the expected molecular weights and low PDIs (Table 1). Absolute molecular weights were determined by triple-detection GPC and by ^{1}H NMR end-group analysis. The results obtained by both methods were found to be consistent and correspond well to the theoretically expected molecular weights. The slower rate of propagation for the formation of PFDES compared to PFDMS is tentatively ascribed to the larger steric demand of the two ethyl substituents on silicon which presumably hinders nucleophilic attack of the propagating anion at the silicon center.

Table 2. Data for PFDES Diblock Copolymers

	M_n first block[a]	block ratio[b]	M_n diblock[b]	PDI[a]
PI_{50}-*b*-$PFDES_{50}$[c]	3 400	1:1	16 900	1.06
PI_{295}-*b*-$PFDES_{54}$	20 100	5.5:1	34 700	1.06
PI_{640}-*b*-$PFDES_{106}$	43 600	6:1	72 200	1.05
PI_{400}-*b*-$PFDES_{29}$	27 200	13:1	35 100	1.04
PI_{368}-*b*-$PFDES_{19}$	25 100	19:1	30 200	1.02

[a] Determined via GPC with THF as eluent. [b] Determined via ^{1}H NMR. [c] Subscripts denoting the degree of polymerization of the corresponding block.

Low-polydispersity polyisoprene-*block*-poly(ferrocenyldiethylsilane) (PI-*b*-PFDES) diblock copolymers were prepared by sequential living anionic polymerization of the respective monomers (see Supporting Information and Chart 2: homopolymers and block copolymers are denoted as, for example, PI$_x$-*b*-PFDES$_y$, where *x* and *y* are the degrees of polymerization for the corresponding blocks). The molecular weight of the first block was determined by gel permeation chromatography, and the block ratio and number of repeat units for each block were calculated by ^{1}H NMR integration (Table 2). The reaction conditions were similar to those used for the PFDMS analogues, and the only difference was the longer polymerization time for the formation of the PFDES block.

2. Morphological Studies of Crystalline PFDES Homopolymer. Prior to studies of the solution self-assembly of the PFDES block copolymers, a detailed investigation of the morphology of the PFDES homopolymer was performed in order to provide a comparison with PFDMS, the well-studied dimethyl analogue.

a. Differential Scanning Calorimetry (DSC) Studies. In an early review on polyferrocenylsilanes the values for the glass transition temperature and the melting point of a PFDES sample with a molecular weight of 4.8 × 10^5 g/mol and a PDI of 1.6 obtained by thermal ROP were reported to be T_g = 22 °C and T_m = 108 °C, respectively.[20] We conducted DSC studies on a series of three low-polydispersity PFDES samples. The glass transition temperatures T_g of all three PFDES homopolymers were obtained in a DSC with heating rates of 10 °C/min. The polymer samples were heated to 200 °C for 30 min followed by rapid quenching to −10 °C prior to the T_g determination. The T_g values of $PFDES_{32}$, $PFDES_{53}$, and $PFDES_{130}$ were found to be 15.0, 18.9, and 22.4 °C, respectively. The increase in T_g with an increase of M_n is well-known for polymers and results from a decrease in the excess free volume associated with the chain ends. A quantitative relation between T_g and M_n was established by Flory and Fox, who reported a linear dependence of $T_g = T_{g,0} + K/M_n$.[22] The respective plot for PFDES is shown in the Supporting Information (Figure S1). Linear regression gives $T_{g,0}$ = 25.0 °C, where $T_{g,0}$ is the glass transition temperature of a polymer sample of infinite molar mass. This value is 8.5 °C lower than the glass transition temperature of PFDMS, $T_{g,0}$ = 33.5 °C.[23] This difference is not surprising. It is well-known that elongation of pendant alkyl chains leads to decreasing glass transition temperatures because the alkyl chains lower the

dx.doi.org/10.1021/ma1029289 |*Macromolecules* 2011, 44, 3777–3786

frictional interaction between the chains and effectively act as "internal diluents".[24]

The melting point of a polymer sample depends on the molecular weight and on the thermal history. The melting traces of the PFDES homopolymers (Figure S2) were determined after 8 h of isothermal annealing at different crystallization temperatures, T_c. In general, the heating scans (10 K/min) revealed more than one endothermic transition. Interestingly, the temperatures of all observed melting peaks were found to be dependent on the isothermal crystallization temperature. This is in contrast to the findings for various PFDMS samples which typically exhibit both a set of peaks that is independent of the isothermal crystallization temperature as well as another set that shows crystallization temperature dependence.[23,25] The most complex melting patterns as well as the most intense melting transitions were found for $PFDES_{32}$, which exhibited up to four melting peaks for the isothermal crystallization at 70 °C. The DSC trace after crystallization for 8 h at 70 °C showed a first melting endotherm with low intensity at 86 °C, which corresponds to a partial melting of the crystals formed during the isothermal crystallization, followed by a more intense endothermic transition at 100 °C where more stable crystallites melt. The occurrence of this peak and the others at higher temperatures (102.5 and 109.8 °C) can tentatively be ascribed to melting and recrystallization of crystallites of different lamellar thickness, with thicker crystallite lamellae formed by recrystallization during the heating scan.[26] The first melting transition was consistently of low intensity for all of the heating scans. This was also true for the samples of $PFDES_{53}$ and $PFDES_{130}$. The DSC traces showed only two endothermic transitions for samples of $PFDES_{53}$ which were crystallized at temperatures below 80 °C and for all of the samples of $PFDES_{130}$.

The value of the first low-intensity melting transition depends linearly on the crystallization temperature for all samples. The position of the melting transitions can be described by the Hoffman–Weeks equation.[27] The Hoffman–Weeks plots for the PFDES homopolymers are shown in the Supporting Information (Figure S2). The melting point for infinite molar mass, $T_{m,0}$, was obtained from the intersection of the extrapolated melting points, T_m, and the crystallization temperature line, T_c, such that $T_m = T_c = T_{m,0}$. For the two polymers of higher molecular weight, i.e. $PFDES_{53}$ and $PFDES_{130}$, a $T_{m,0}$ value of 138 °C was obtained, whereas the value for $PFDES_{32}$ obtained by this method (124 °C) was significantly lower. The value of the equilibrium melting point as determined by the Hoffman–Weeks equation, $T_{m,0}$ = 138 °C, is higher than the previously reported melting point of T_m = 108 °C, which had been obtained from a single DSC trace of a polydisperse sample.[20] On the other hand, the melting point is lower than the melting point of PFDMS (145 °C) obtained from the Hoffman–Weeks equation.[23,25] This trend is in accordance with other crystalline polymers such as isotactic poly(α-olefins) whose melting point decreases from polypropylene to poly(1-pentene).[28]

In order to compare the melt enthalpies for PFDES and PFDMS, two identically treated samples (isothermal crystallization at 80 °C for 8 h) of comparable molecular weight, $PFDES_{53}$ and $PFDMS_{51}$, were studied. The values were found to be 21.0 J/g for $PFDES_{53}$ and 14.9 J/g for $PFDMS_{51}$. This indicates a higher melt enthalpy for the PFDES sample. Rehahn and co-workers recently reported values of 19.3 J/g for $PFDMS_{20}$ and 14.7 J/g for $PFDMS_{250}$.[29] Considering the difference in sample preparation (annealing was performed at temperatures around 120 °C for more than 60 h), their results are in good agreement with our data.

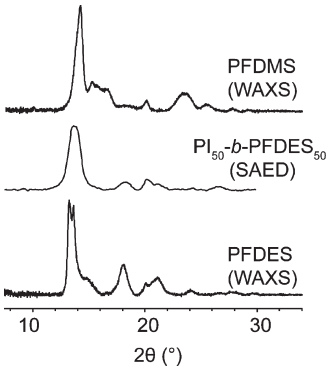

Figure 1. WAXS patterns of $PFDMS_{51}$ (top) and $PFDES_{53}$ (bottom) crystallized from hexane/THF and SAED pattern of PI_{50}-*b*-$PFDES_{50}$ crystallized from decane/xylene at 50 °C.

Table 3. *d*-Spacings of Solution-Crystallized $PFDES_{53}$, PI_{50}-*b*-$PFDES_{50}$, and $PFDMS_{51}$ Obtained from WAXS and SAED Data

$PFDES_{53}$[a]	PI_{50}-*b*-$PFDES_{50}$[b]	$PFDMS_{51}$[a]
0.67[c]		0.63[c]
0.65[c]	0.65[c]	0.59
0.60		0.54
0.49	0.49	0.44
0.44	0.44	0.38
0.42	0.42	0.35
0.37		0.32
0.33	0.34	
0.32		

[a] From WAXS data. [b] From SAED data. [c] Most intense peaks.

b. Studies of Solution- and Melt-Crystallized Samples of PFDES. In order to obtain more detailed information on the crystallization of PFDES, we prepared a sample of $PFDES_{53}$ from solution by dissolving 24 mg of $PFDES_{53}$ in 6 mL of THF followed by the addition of 18 mL of hexane. After 18 h the polymer had precipitated out of solution, and the resulting amber powder was subjected to a wide-angle X-ray scattering (WAXS) analysis. For comparison, a crystalline sample of $PFDMS_{51}$ was prepared analogously. Both diffractograms are depicted in Figure 1. The diffraction patterns of PFDES and PFDMS are similar in shape, but the most intense peaks arise at slightly different *d*-spacing (Table 3). The two major differences for the two polymers are, first, the splitting of the most intense peak in the PFDMS diffractogram at a *d*-spacing of 0.63 nm into two resolved peaks at 0.67 and 0.65 nm for PFDES and, second, the occurrence of an intense peak at 0.49 nm in the PFDES diffractogram. The crystallinity of $PFDES_{53}$ was estimated via integration of the obtained WAXS pattern after subtraction of the amorphous halo (Figure S3) and was found to be around 62%. This is higher than the reported value for PFDMS, which was 48%,[30] and is consistent with the conclusion based on DSC studies, that PFDES has a higher melting enthalpy (section 2a).

We also conducted AFM studies on samples crystallized from the melt. Figure 2 shows AFM images of a $PFDES_{130}$ sample

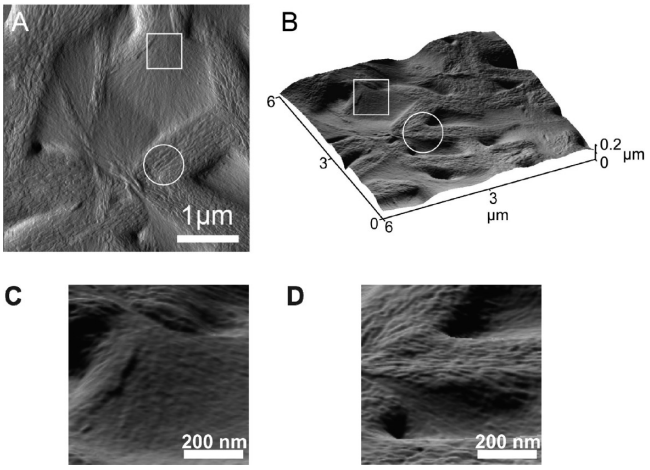

Figure 2. (A) AFM deflection image (*z*-range 60 mV) and (B) rendered height image of a $PFDES_{130}$ thin film crystallized at 80 °C for 24 h. Enlargements of regions depicted by a square (C) and circle (D) are shown in higher magnification.

which was spin-cast from a 20 mg/mL toluene solution onto a Si wafer to give a ca. 150 nm thick film which was subsequently crystallized at 80 °C for 24 h. A $PFDES_{53}$ sample which was crystallized following the same protocol showed essentially the same features. The influence of the crystallization temperature was also studied, but no significant morphological differences were found by crystallizing $PFDES_{53}$ at 60 °C instead of 80 °C, whereas $PFDES_{130}$ showed few crystalline structures after 24 h at 60 °C. The morphology obtained for $PFDES_{130}$ crystallized at 80 °C for 24 h consisted mainly of sheaf-like aggregates of edge-on lamellae which appear to be slightly tilted in some areas (see Figure 2, with selected regions enlarged in Figure 2C,D). Hedritic structures were also detected in analogous studies of melt-crystallized samples of PFDMS.[25]

3. Solution Self-Assembly of PI-*b*-PFDES Diblock Copolymers. *a. Formation of Cylinders and Platelets with a Crystalline PFDES Core.* It is well established that PFDMS block copolymers (such as PI-*b*-PFDMS, PFDMS-*b*-P2VP, or PFDMS-*b*-PDMS), with a remarkably wide range of block ratios, form cylindrical micelles with a semicrystalline PFDMS core in selective solvents for the complementary block.[12a,31] We investigated whether analogous PFDES diblock copolymers would undergo similar self-assembly behavior by studying several PI-*b*-PFDES diblock copolymers.

Our initial work involved PI_{295}-*b*-$PFDES_{54}$ (block ratio 6:1), since the PFDMS analogue gives well-defined cylinders in selective solvents for the PI block under a range of different conditions.[31b] However, dissolution of PI_{295}-*b*-$PFDES_{54}$ in hexane at 60 °C, a standard protocol for the generation of worm-like PI-*b*-PFDMS micelles, only gave one-dimensional objects with irregular edges and a nonuniform width, according to TEM analysis (Figure S4). To ensure that the polymer chains would be dissolved as unimers before undergoing self-assembly, we prepared a 10 mg/mL solution of PI_{295}-*b*-$PFDES_{54}$ in THF, a common solvent for each block, and added 25 μL of this solution to 500 μL of stirred *n*-hexane which is a selective solvent for polyisoprene. Subsequent TEM analysis of the aged sample (1 day) revealed the formation of cylindrical PI_{295}-*b*-$PFDES_{54}$ micelles (Figure 3A). Interestingly, the micelles obtained were again not as well-defined as their PI-*b*-PFDMS analogues. It is clear from the inspection of the TEM

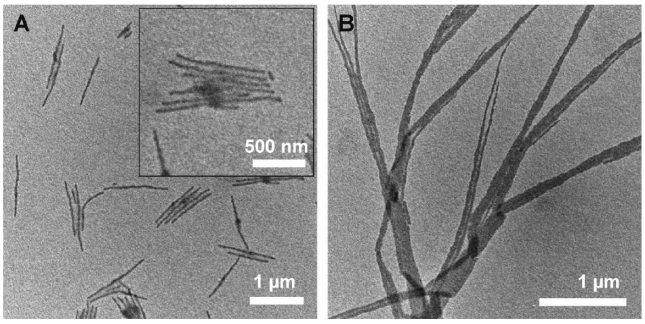

Figure 3. TEM micrographs of self-assembled PI_{295}-*b*-$PFDES_{54}$ structures which were prepared using different protocols: (A) To 500 μL of hexane was added 25 μL of PI_{295}-*b*-$PFDES_{54}$ (10 mg/mL in THF) with stirring; the inset shows cylinders at higher magnification. (B) 2.1 mg of PI_{295}-*b*-$PFDES_{54}$ in 21 mL of decane/xylene (9:1 v/v) was heated to 100 °C and then aged for 1 day at room temperature.

micrograph in Figure 3A that a fraction of the cylinders possessed a thicker central region. The cylinders were characterized by a number-average length of L_n = 518 nm and a non-uniform width that diminished from up to 30 nm in the center of the micelle to 12 nm at the ends. Dynamic light scattering (DLS) measurements at a scattering angle of 173° indicated a bimodal distribution of species in solution (Figure S6) and values for the apparent hydrodynamic radius ($R_{h,app}$) ranging from 105 to 412 nm. These values are qualitatively consistent with the distribution of objects determined in the TEM after solvent removal.

Surprisingly, by changing the solvent system and the crystallization protocol, we were able to change the self-assembled morphology from cylindrical micelles with thicker internal regions to tape-like structures. Dissolution of 2.1 mg of PI_{295}-*b*-$PFDES_{54}$ in a mixture of 21 mL of the selective solvent decane and the common solvent xylene (9:1 v/v) at 100 °C for 1 h and subsequent aging at room temperature afforded a clear solution which contained bundles of tape-like PI_{295}-*b*-$PFDES_{54}$ crystals (Figure 3B; for corresponding AFM data and thickness measurements see Figure S5 and Table S1). These tapes possessed lengths of up to 10 μm and widths between 14 nm at the ends and 350 nm in the middle. Similar results were obtained when the block copolymer was dissolved in THF and hexane was added extremely slowly. The self-assembly conditions that were found to favor the formation of more tape-like structures involved higher dilution, a higher fraction of a common solvent for both blocks, and a higher initial temperature and would therefore be expected to involve a slower and more extensive crystallization of the core forming PFDES block.

The self-assembly of PI_{640}-*b*-$PFDES_{106}$, another PI-*b*-PFDES diblock copolymer with a block ratio of ca. 6:1 but with approximately double the overall molecular weight, gave results that were similar to those for PI_{295}-*b*-$PFDES_{54}$. Heating of 2.0 mg of PI_{640}-*b*-$PFDES_{106}$ in 4 mL of decane to 100 °C for 1 h yielded a clear pale-yellow solution. Cylindrical objects formed when this solution was cooled down rapidly (10 °C/min) to room temperature and allowed to age for 1 day (Figure 4A). Again, the central region of a large fraction of the cylinders was somewhat thicker than the ends of the cylinder. The cylinders were characterized by an average length of L_n = 563 nm and widths that ranged from 12 nm at the ends up to 40 nm in the center of the micelle. Much longer tape-like structures formed when 1.7 mg of the same polymer PI_{640}-*b*-$PFDES_{106}$ was heated to 100 °C in 17 mL of decane/xylene

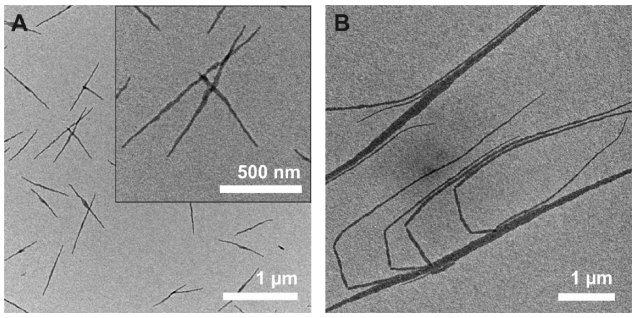

Figure 4. TEM micrographs of self-assembled PI_{640}-*b*-$PFDES_{106}$ structures which were prepared using different protocols: (A) 2 mg of PI_{640}-*b*-$PFDES_{106}$ was heated in 4 mL of decane to 100 °C for 1 h and cooled down at ~10 °C/min to room temperature; the inset shows a higher magnification. (B) 1.7 mg of PI_{640}-*b*-$PFDES_{106}$ was heated in 17 mL of decane/xylene (9:1) to 100 °C for 1 h and then aged at room temperature for 24 h.

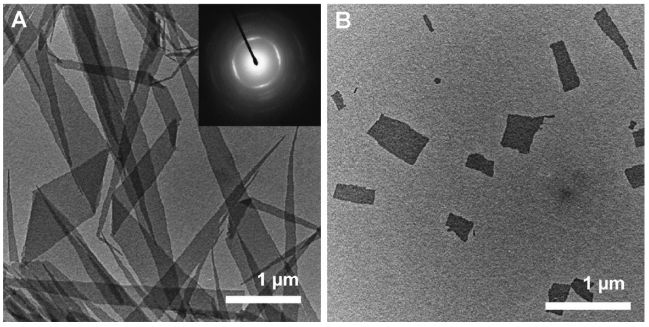

Figure 5. TEM micrograph of (A) tape-like structures obtained from self-assembly of PI_{50}-*b*-$PFDES_{50}$, 1.1 mg of the diblock copolymer was dissolved in 11 mL of decane/xylene (10:1 v/v) at 100 °C for 1 h, kept at 60 °C for 4 h, aged at 50 °C for 18 h, followed by cooling to RT. The inset shows the SAED pattern. (B) Platelets of PI_{50}-*b*-$PFDES_{50}$ formed by sonication (10 min in an ultrasonic bath).

(9:1 v/v) for 1 h, and the resulting solution was then kept at room temperature for another 24 h. TEM analysis of the solution revealed long (>10 μm) and branched tape-like structures (Figure 4B; for corresponding AFM data and thickness measurements see Figure S5 and Table S1). Their widths ranged from 170 nm in the central region to 14 nm at the ends. Clearly, a combination of higher dilution (0.1 mg/mL) and the presence of a common solvent (xylene) for both blocks again favored the formation of longer tape-like structures compared to the much shorter and more regular cylinder-like objects which form at higher concentration (0.5 mg/mL) in the absence of a common solvent.

It has been previously reported that PI-*b*-PFDMS diblock copolymers form tape-like structures at block ratios of 1:2 and 1:1.[12b] In contrast, PI-*b*-PFDES diblock copolymers with a block ratio of 6:1 formed either cylindrical structures with plate-like central regions or tape-like structures depending on the crystallization conditions. In a similar manner to the PI-*b*-PFDMS system, PI-*b*-PFDES with a 1:1 block ratio was found to exclusively form tape-like structures. When 1.1 mg of PI_{50}-*b*-$PFDES_{50}$ was dissolved in 11 mL of decane/xylene (10:1 v/v) at 100 °C for 1 h, then kept at 60 °C for 4 h, followed by additional aging at 50 °C for 18 h, aggregates of tape-like structures with lengths of more than 10 μm and widths up to 900 nm in the central region of the tapes were formed (Figure 5A; for

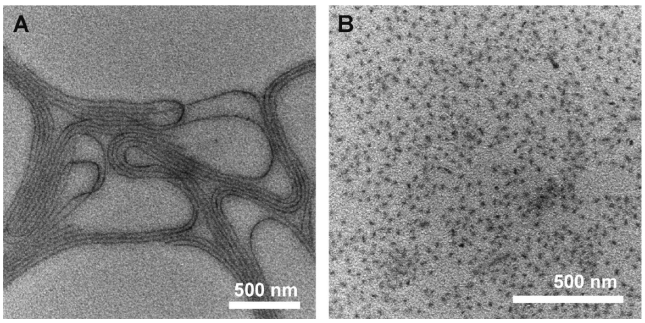

Figure 6. TEM micrograph of a solution of (A) PI_{368}-*b*-$PFDES_{19}$ which was heated in *n*-hexane (1 mg/mL) to 60 °C for 1 h, then cooled to RT and aged for 1 month, and (B) stub-like objects which are obtained by ultrasound treatment of (A) for 4 h at −78 °C.

corresponding AFM data and thickness measurements see Figure S5 and Table S1).

The crystalline nature of the PFDES core of these tape-like objects was also studied by selected area electron diffraction (SAED). For this experiment, self-assembly was carried out by dissolving 1.1 mg of PI_{50}-*b*-$PFDES_{50}$ at 100 °C in a mixture of 11 mL of decane/xylene (10:1 v/v) and subsequent crystallization for 4 h at 60 °C and an additional 18 h at 50 °C. The diffraction peaks were found to correspond well to the WAXS data obtained from the $PFDES_{53}$ homopolymer (see Figure 1), which indicated that the crystalline PFDES regions in the PI_{50}-*b*-$PFDES_{50}$ diblock copolymer micelles are structurally very similar to crystallites present in PFDES homopolymer.

The tape-like structures formed by PI_{50}-*b*-$PFDES_{50}$ were found to be fragmented by exposure to ultrasound. Thus, a 2 mL aliquot was sonicated for 10 min in an ultrasonic bath. Platelet-like objects with a similar width as the tape-like structures but much shorter lengths of L_n = 470 nm (L_w/L_n = 1.42) were found (Figure 5B). This suggests that cleavage occurs preferentially along the long axis of the tapes. It has been previously shown that the rate of fragmentation of cylindrical micelles with a PFDMS core is highly dependent on the length of the micelles with the rate constant $k_{frag} \sim l^{2.6}$, which supports preferential cleavage of the tape-like structures along their long axis.[32] For tape-like architectures, however, an influence of different crystal packing along the different directions would also be anticipated.

The cylindrical structures that were obtained by self-assembly of PI-*b*-PFDES diblock copolymers with a 6:1 block ratio had thicker central regions and were rather short (500 nm). In an attempt to obtain more regular cylindrical micelles, we synthesized a PI-*b*-PFDES diblock copolymer with a much shorter $PFDES_{19}$ block and a block ratio of 19:1. We anticipated that the repulsion of the longer coronal PI chains should promote curvature of the core−corona interface to counter the influence of PFDES crystallization on self-assembly.[12] The dissolution of this new diblock copolymer, PI_{368}-*b*-$PFDES_{19}$, at 60 °C in hexane (a standard protocol for the self-assembly for PI-*b*-PFDMS diblock copolymers which failed to give well-defined cylinders for PI_{295}-*b*-$PFDES_{54}$) gave very long and well-defined cylindrical micelles after the sample was aged for 1 month at room temperature (Figure 6A). Clearly, the self-assembly of PI_{368}-*b*-$PFDES_{19}$ is extremely slow compared to, for example, PI_{295}-*b*-$PFDES_{54}$, where aging for 1 day was found to be sufficient. After only 1 day TEM showed only a small fraction of very short cylindrical objects (Figure S7). The cylindrical

Table 4. Length Analysis of the Cylindrical Micelles Grown from PI_{368}-*b*-$PFDES_{19}$ Seeds for Different Amounts of Added Unimers of PI_{295}-*b*-$PFDES_{54}$

	mass ratio: $m_{unimers}/m_{seeds}$ [a]				
	seed	1.25	2.5	5	10
L_n (nm)	18	65	125	197	346
L_w (nm)	19	71	133	208	358
L_w/L_n	1.06	1.09	1.06	1.06	1.03
σ/L_n	0.23	0.30	0.25	0.23	0.19

[a] m_{seeds}: total mass of seed crystals in the seed solution; $m_{unimers}$: total mass of unimers added.

micelles formed after aging for 1 month were longer than 3 μm and around 10 nm wide. They were also fractured by ultrasound. Figure 6B shows the TEM micrograph of the resulting stub-like objects which are obtained when a cooled vial (−78 °C) with the solution was sonicated for 4 h with a sonotrode attached to a 50 W ultrasound processor. These stubs were on average L_n = 18 nm long and 10 nm wide (Table 4). Similar behavior has been reported for analogous PFDMS block copolymers.[15]

The block length ratios of PI:PFDES discussed so far were either 1:1 (which gave platelets, Figure 5), 6:1 (forming ill-defined cylinders or tapes, Figures 3 and 4), or 19:1 (resulting in well-defined cylinders, Figure 6). For comparison, we also synthesized a block copolymer of an intermediate composition, PI_{400}-*b*-$PFDES_{29}$, with a block ratio of 13:1. Self-assembly of this block copolymer in hexanes (1 g/L, heated to 60 °C for 1 h, afterward aged at RT for 3 days) yielded cylindrical micelles which were neither as ill-defined as for the 6:1 materials nor as well-defined as for a ratio of 19:1. Furthermore, the rate of self-assembly appeared to be in between that detected for PI_{295}-*b*-$PFDES_{54}$ (1 day) and PI_{368}-*b*-$PFDES_{19}$ (1 month). A representative TEM micrograph after aging for 3 days is shown in Figure S8.

b. Crystallization-Driven Living Self-Assembly of PFDES Block Copolymers. It is desirable to have access to 1-dimensional nanostructures such as cylindrical micelles with tunable length and low length dispersity.[15] We have recently shown that cylindrical micelles with semicrystalline PFDMS cores undergo seeded crystallization-driven living self-assembly which enables length control and yields monodisperse cylindrical nanostructures.[13−15] Since this process is crystallization-driven, we expected that cylindrical micelles with a semicrystalline PFDES core should exhibit similar behavior under appropriate conditions. We used the stub-like seeds of PI_{368}-*b*-$PFDES_{19}$ (block ratio ∼19:1) micelles as a seed material (Figure 6B). Unfortunately, the seeded self-assembly of PI_{368}-*b*-$PFDES_{19}$ is extremely slow and takes 1 month for the growth process to reach completion. We therefore used PI_{295}-*b*-$PFDES_{54}$ (block ratio ∼6:1) as the second-stage building block. This polymer self-assembles more rapidly (over 1 day).

To carry out these experiments, we prepared 2 mL aliquots of a 0.05 mg/mL solution of the stub-like seeds of PI_{368}-*b*-$PFDES_{19}$ in hexane and added different amounts (12.5, 25, 50, and 100 μL) of a THF solution of PI_{295}-*b*-$PFDES_{54}$ (10 mg/mL) to each seed solution. These solutions were allowed to age for 1 day. Contin plots from DLS measurements (Figure S9) show that that the apparent hydrodynamic radii increased with the amount of free polymer added. TEM micrographs of the resulting cylindrical micelles are shown in Figure 7. A length analysis was carried out by measuring the length of more than 400 micelles per sample using

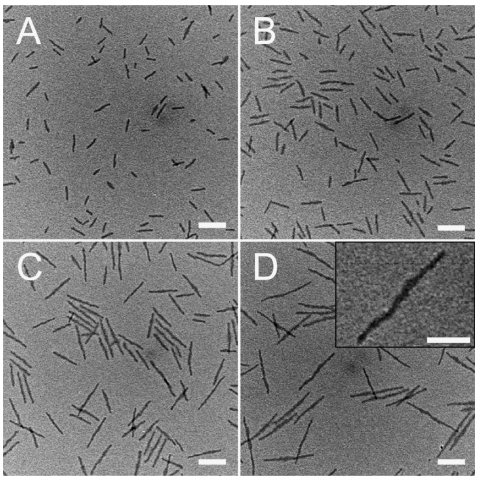

Figure 7. TEM micrographs of cylindrical micelles of PI_{295}-*b*-$PFDES_{54}$ formed by adding (A) 12.5, (B) 25, (C) 50, and (D) 100 μL of a 10 mg/mL THF solution of PI_{295}-*b*-$PFDES_{54}$ to 2 mL of a 0.05 mg/mL hexane solution of stub-like seeds of PI_{368}-*b*-$PFDES_{19}$. The inset in (D) shows that the cylinders are not perfectly straight; scale bars correspond to 100 nm.

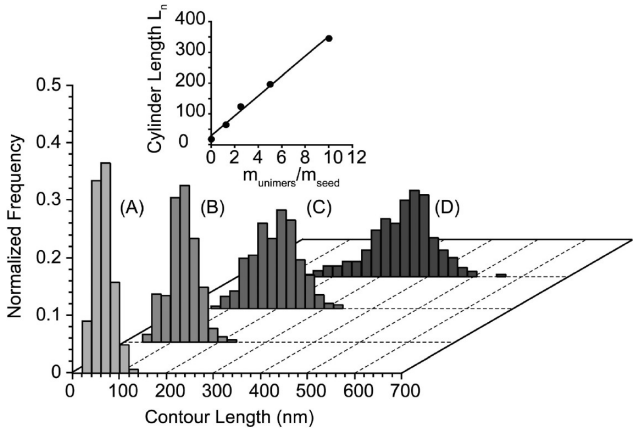

Figure 8. Histograms of the length distribution of the cylindrical micelles formed by adding (A) 12.5, (B) 25, (C) 50, and (D) 100 μL of a 10 mg/mL THF solution of PI_{295}-*b*-$PFDES_{54}$ to 2 mL of a 0.05 mg/mL hexane solution of stub-like seeds of PI_{368}-*b*-$PFDES_{19}$ with L_n = 18 nm.

ImageJ software. Table 4 lists the values for L_n, L_w, and L_w/L_n and also the standard deviations (σ/L_n) for all of the samples. The values for σ/L_n were calculated according to eq S3 (Supporting Information). Histograms of the cylinder length distributions are shown in Figure 8. The lengths of the seeded cylinders were found to depend linearly on the ratio of the amount of unimers to the seeds (inset, Figure 8). The length distributions were narrow, with L_w/L_n values between 1.09 for the shortest seeded cylinders (L_n = 65 nm) and 1.03 for the longest cylinders (L_n = 346 nm).

After the addition of 50 and 100 μL of the unimer solution, it was clear from subsequent TEM analysis that the resulting cylinders were not as uniform and well-defined as in case of the analogous PFDMS materials (see inset in Figure 7D). Moreover, the values obtained for L_w/L_n and the standard deviation, σ/L_n, confirmed the controlled growth of the cylinders but were found to be significantly larger compared those for the analogous PFDMS block copolymers.[15]

dx.doi.org/10.1021/ma1029289 |*Macromolecules* 2011, 44, 3777–3786

c. Attempted Heteroepitaxial Growth Experiments with PFDMS and PFDES Block Copolymers. We have recently shown that the coil−crystalline block copolymer polyisoprene-*block*-poly(ferrocenyldimethylgermane) (PI-*b*-PFDMG) can be grown in a controlled fashion from PI-*b*-PFDMS seed micelles, resulting in cylindrical block comicelles with different core-forming blocks.[16] We therefore investigated whether the addition of block copolymer unimers of PI_{332}-*b*-$PFDMS_{29}$ (block ratio = 11:1) to preformed seed micelles of PI_{368}-*b*-$PFDES_{19}$ (block ratio = 19:1) (Figure 6B) results in a controlled extension to form cylindrical micelles. We added 100 μL of a 10 g/L solution of PI_{332}-*b*-$PFDMS_{29}$ to 2 mL of a 0.05 g/L solution of the stub micelles in *n*-hexane with vigorous stirring, and the solution was subsequently aged for several days. TEM analysis subsequently showed that the PI_{368}-*b*-$PFDES_{19}$ stub micelles were still present and, additionally, also revealed the formation of long cylindrical micelles (Figure S10A). The long micelles were comparable to those reported earlier for PI-*b*-PFDMS block copolymers under similar conditions and are believed to result from homonucleation of the PFDMS segments.[13] An analogous experiment but in reverse was performed using PI_{332}-*b*-$PFDMS_{29}$ seed micelles (block length ratio 11:1) where 100 μL of a 10 g/L solution of PI_{368}-*b*-$PFDES_{19}$ (block ratio = 19:1) in THF were added to 2 mL of a 0.05 g/L solution of the seeds. As a result of the rather slow self-assembly of the latter block copolymer noted earlier, this sample was aged for 2 weeks prior to TEM analysis. A representative micrograph is shown in Figure S10B. Similar to the situation illustrated in Figure S10A, both remaining stub micelles and newly formed, distinctly larger objects, presumably cylinders formed by homonucleation of PI_{368}-*b*-$PFDES_{19}$, were observed.

Clearly, the direct epitaxial growth of PFDES from PFDMS seed micelles (and vice versa) is not possible, at least not under the conditions studied in this work. One explanation could be that the homonucleation/homoepitaxy of the added block copolymer unimers is much faster when compared to the heteroepitaxial growth onto the facets of the stub micelles already present in solution. To investigate this possibility further, 100 μL of a PI_{368}-*b*-$PFDES_{19}$ solution (10 g/L) in THF was added extremely slowly to 2 mL of a 0.05 g/L solution of PI_{332}-*b*-$PFDMS_{29}$ seed micelles in hexane with a syringe pump over 20 h. Again, both remaining seed micelles and newly generated long PI_{368}-*b*-$PFDES_{19}$ cylindrical micelles could be detected by TEM. This suggests that the differences between the lattices of PFDMS and PFDES is the major factor hindering heteroepitaxial growth, despite a difference of only about 6% between the most pronounced peaks in the WAXS patterns at 0.63 nm (for PFDMS) and 0.67 nm (for PFDES).

DISCUSSION

The results described above illustrate that the apparently subtle change from methyl groups on silicon in PFDMS to ethyl substituents in PFDES leads to both analogous and significantly different self-assembly behavior for the respective PI-*b*-PFS block copolymers in solution. Our detailed DSC and WAXS studies of PFDES homopolymer also allowed comparisons with similar data for the PFDMS analogue (sections 2a and 2b). The results indicated that the former material possesses a significantly higher melt enthalpy and degree of crystallinity than the latter.

The self-assembly of PI-*b*-PFDES block copolymers in a PI selective solvent revealed an ability to form non-spherical morphologies characterized by a lower degree of interfacial curvature, such as cylinders and platelets. This behavior is reminiscent to that observed for PI-*b*-PFDMS.[12a] However, the balance between crystallinity and coronal chain repulsion that we previously proposed to explain the formation of cylinders for the latter material at a block ratio of ca. 6:1[12b] appears to be significantly shifted in the case of PI-*b*-PFDES. Thus, a similar block ratio of 6:1 yields platelets, tape-like structures, or cylinders with thicker plate-like internal sections, and well-defined cylinders were only formed for substantially more asymmetric compositions (i.e., 19:1, see section 3a, Figure 6; an intermediate composition (13:1) gave slightly non-uniform cylindrical micelles). This behavior is consistent with the higher melt enthalpy and degree of crystallinity of the PFDES block leading to the emergence of crystallization as a more dominant factor. Thus, the presence of longer coronal blocks with their more substantial associated interchain repulsions is necessary to allow the formation of morphologies such as cylinders, which possess an interfacial curvature that is intermediate between that of platelets or tapes and spheres.

Another interesting feature of the PI-*b*-PFDES block copolymers with short PFDES blocks is their much decreased rate of self-assembly. For example, PI_{368}-*b*-$PFDES_{19}$ requires ca. 1 month for the unimers to be completely consumed. This appears to be the result of the slow deposition and crystallization of the PFDES core-forming block under these conditions. Although any explanation can only be speculative at this point, it is possible that partial coverage of the exposed cores at the ends of the cylinders by the long PI corona-forming block may be the cause of the decrease of the rate of unimer addition for PI_{368}-*b*-$PFDES_{19}$. Studies of highly asymmetric block copolymers such as $PFDMS_{54}$-*b*-$PDMS_{945}$ in selective solvents for the PDMS co-block also show very slow self-assembly rates, and a similar explanation may operate in this case.[33]

Despite the significant differences in behavior noted for the PI-*b*-PFDES block copolymers compared to their PFDMS analogues, similar[13,15] crystallization-driven living self-assembly was successfully demonstrated for the growth of cylinders by the addition of unimers of PI_{295}-*b*-$PFDES_{54}$ to stub-like seeds of PI_{368}-*b*-$PFDES_{19}$ generated by sonication. Although the resulting cylindrical micelles are less well-defined than their PFDMS analogues, this provided a further example of where cylinders can be successfully templated for block copolymers that tend to yield less regular structures by direct self-assembly processes.[16] Nevertheless, attempts to achieve heteroepitaxial growth by the addition of PI-*b*-PFDMS to seeds of PI-*b*-PFDES (and vice versa) were unsuccessful. Our results indicate that the crystal lattices of PFDMS and PFDES are insufficiently similar despite the relatively small (ca. 6%) difference in the *d*-spacings of the most intense peaks in the WAXS patterns (see section 2b). This observation stands in contrast to our previous finding of growth of PFDMG block copolymer unimers from seed micelles with PFDMS cores, where there was a similarly small mismatch in the lattice *d* spacings.[16] Kinetic factors may also play a role in suppressing heteroepitaxial growth for the PI-*b*-PFDMS + PI-*b*-PFDES system. One starting point for future work might be the study of the analogous behavior of block copolymers with gradient or tapered blocks consisting of both $fcSiMe_2$ and $fcSiEt_2$ repeat units (fc = $Fe(\eta\text{-}C_5H_4)_2$). Detailed investigations of their self-assembly and attempts to template PFDES and PFDMS block copolymers from seeds of these materials (and vice versa) at different compositions may allow us to successfully circumvent the problems with the PI-*b*-PFDMS/PI-*b*-PFDES heteroepitaxial growth apparent in this study. This approach would be analogous to the use of compatibilizing layers in semiconductor heteroepitaxy.[34]

SUMMARY

The process of crystallization-driven living self-assembly illustrated by PFDMS block copolymers represents a promising new approach to well-defined cylinders and hierarchical architectures.[13,15,16] We have now shown that PI-*b*-PFDES diblock copolymers with a semicrystalline PFDES core-forming block exhibit both similarities and important differences in their solution self-assembly behavior compared to their well-studied PFDMS counterparts. An important difference was the more pronounced tendency of PI-*b*-PFDES diblock copolymers to form morphologies with lower interfacial curvature. Thus, uniform cylindrical structures were obtained only by increasing the PI:PFDES block ratio to 19:1. In comparison, the PFDMS analogues self-assemble to form cylinders at much lower block ratios (down to 5:1). This behavior has been attributed to the higher melt enthalpy and degree of crystallinity of PFDES compared to PFDMS. Interestingly, highly asymmetric PI-*b*-PFDES block copolymers, such as the material with a 19:1 block ratio and, to a lesser extent, the analogous copolymer with a ratio of 13:1, were characterized by a very slow rate of self-assembly. Restricted accessibility of the PFDES core at the ends of the micelles due to partial coverage by the long PI coronal chains may provide the explanation for this behavior.

As with the case of the PFDMS analogues, the length of cylindrical PI−PFDES block copolymer micelles could be controlled by a crystallization-driven living self-assembly process by using stub-like seeds as initiators. The successful extension of living self-assembly to diblock copolymers with a PFDES core-forming block suggests that this process may be applicable to a range of diblock copolymers with a semicrystalline core, potentially including all-organic materials. However, the results reported here also indicate that different crystallization behavior may require modified block ratios to achieve the desired morphologies via living self-assembly. Furthermore, although our attempts to establish protocols for the heteroepitaxial growth for the PFDMS/PFDES combination have proven to be unsuccessful, we note that this has been achieved in the case of PFDMS/PFDMG interfaces.[16] We are currently investigating the use of core-forming PFS blocks that contain a random distribution of $SiMe_2$ and $SiEt_2$ groups. By analogies with the techniques of semiconductor heteroepitaxy, this may allow us to deposit compatibilizing layers that subsequently allow successful heteroepitaxial growth between the PFDMS and PFDES core-forming blocks.[34]

ASSOCIATED CONTENT

Supporting Information. Experimental details, DSC scans, Hoffman−Weeks plots for different PFDES samples, AFM data, and additional figures. This material is available free of charge via the Internet at http://pubs.acs.org.

AUTHOR INFORMATION

Corresponding Author

*E-mail: ian.manners@bristol.ac.uk (I.M.); mwinnik@chem.utoronto.ca (M.A.W.).

Present Addresses

[§]Laboratory of Organic and Macromolecular Chemistry and Jena Center for Soft Matter, Friedrich-Schiller-University Jena, Humboldtstrasse 10, D-07743 Jena, Germany.

ACKNOWLEDGMENT

The authors thank the European Union for financial support. T.G. (DFG) and F.H.S. (DAAD) are grateful for a postdoctoral fellowship. I.M. thanks the European Union for a Marie Curie Chair, the European Research Council for an Advanced Investigator Award, and the Royal Society for a Wolfson Research Merit Award. We also thank J. Mitchels for helpful discussions and assistance during the AFM measurements. M.A.W. thanks NSERC (Canada) for financial support. We also thank Dr. Paul Rupar for drawing Scheme 1.

REFERENCES

(1) (a) Gohy, J.-F. *Adv. Polym. Sci.* **2005**, *190*, 65. (b) Lazzari, M.; López-Quintela, M. A. *Adv. Mater.* **2003**, *15*, 1583. (c) Discher, D. E.; Eisenberg, A. *Science* **2002**, *297*, 967. (d) Won, Y.-Y.; Davis, H. T.; Bates, F. S. *Science* **1999**, *283*, 960. (e) Jain, S.; Bates, F. S. *Science* **2003**, *300*, 460. (f) Savic, R.; Luo, L.; Eisenberg, A.; Maysinger, D. *Science* **2003**, *300*, 615. (g) Hu, J.; Liu, G.; Nijkang, G. *J. Am. Chem. Soc.* **2008**, *130*, 3236. (h) Kim, Y.; Dalhaimer, P.; Christian, D. A.; Discher, D. E. *Nanotechnology* **2005**, *16*, 484. (i) Cao, L.; Massey, J. A.; Winnik, M. A.; Manners, I.; Riethmüller, S.; Banhart, F.; Spatz, J. P.; Möller, M. *Adv. Funct. Mater.* **2003**, *13*, 271. (j) Geng, Y.; Dalhaimer, P.; Cai, S.; Tsai, R.; Tewari, M.; Minko, T.; Discher, D. E. *Nature Nanotechnol.* **2007**, *2*, 249.

(2) (a) Zhang, L.; Eisenberg, A. *Science* **1995**, *268*, 1728. (b) Zhang, L.; Yu, K.; Eisenberg, A. *Science* **1996**, *272*, 1777. (c) Abbas, S.; Li, Z.; Hassan, H.; Lodge, T. P. *Macromolecules* **2007**, *40*, 4048. (d) Yuan, J.; Xu, Y.; Walther, A.; Bolisetty, S.; Schumacher, M.; Schmalz, H.; Ballauff, M.; Müller, A. H. E. *Nature Mater.* **2008**, *7*, 718.

(3) (a) Pochan, D. J.; Chen, Z.; Cui, H.; Hales, K.; Qi, K.; Wooley, K. L. *Science* **2004**, *306*, 94. (b) Cui, H.; Chen, Z.; Zhong, S.; Wooley, K. L.; Pochan, D. J. *Science* **2007**, *317*, 647. (c) Li, Z.; Kesselman, E.; Talmon, Y.; Hillmyer, M. A.; Lodge, T. P. *Science* **2004**, *306*, 98. (d) Schacher, F.; Walther, A.; Ruppel, M.; Drechsler, M.; Müller, A. H. E. *Macromolecules* **2009**, *42*, 3540. (e) Zhu, J.; Jiang, W. *Macromolecules* **2005**, *38*, 9315. (f) Dupont, J.; Liu, G.; Niihara, K.-I.; Kimoto, R.; Jinnai, H. *Angew. Chem., Int. Ed.* **2009**, *48*, 6144. (g) Hu, J.; Njikang, G.; Liu, G. *Macromolecules* **2008**, *41*, 7993.

(4) (a) Lotz, B.; Kovacs, A. J.; Bassett, G. A.; Keller, A. *Colloid Polym. Sci.* **1966**, *209*, 115. (b) Lotz, B.; Kovacs, A. J. *Colloid. Polym. Sci.* **1966**, *209*, 97.

(5) (a) Richter, D.; Schneiders, D.; Monkenbusch, M.; Willner, L.; Fetters, L. J.; Huang, J. S.; Lin, M.; Mortensen, K.; Farago, B. *Macromolecules* **1997**, *30*, 1053. (b) Ramzi, A.; Prager, M.; Richter, D.; Efstratiadis, V.; Hadjichristidis, N.; Young, R. N.; Allgaier, J. B. *Macromolecules* **1997**, *30*, 7171. (c) Lin, E. K.; Gast, A. P. *Macromolecules* **1996**, *29*, 4432. (d) Vilgis, T.; Halperin, A. *Macromolecules* **1991**, *24*, 2090.

(6) Gast, A. P.; Vinson, P. K.; Cogan-Farinas, K. A. *Macromolecules* **1993**, *26*, 1774.

(7) (a) Kulbaba, K.; Manners, I. *Macromol. Rapid Commun.* **2001**, *22*, 711. (b) Bellas, V.; Rehahn, M. *Angew. Chem., Int. Ed.* **2007**, *46*, 5082. (c) Whittell, G. R.; Hager, M. D.; Schubert, U. S.; Manners, I. *Nature Mater.* **2011**, *10*, 176.

(8) (a) Li, J. K.; Zou, S.; Rider, D. A.; Manners, I.; Walker, G. C. *Adv. Mater.* **2008**, *20*, 1989. (b) Eitouni, H. B.; Balsara, N. P. *J. Am. Chem. Soc.* **2006**, *128*, 16248. (c) Rider, D. A.; Winnik, M. A.; Manners, I. *Chem. Commun.*, **2007**, *43*, 4483.

(9) (a) Korczagin, I.; Lammertink, R. G. H.; Hempenius, M. A.; Golze, S.; Vancso, G. J. *Adv. Polym. Sci.* **2006**, *200*, 91. (b) Rider, D. A.; Chen, J. I. L.; Eloi, J.-C.; Arsenault, A. C.; Russell, T. P.; Ozin, G. A.; Manners, I. *Macromolecules* **2008**, *41*, 2250. (c) Datta, U.; Rehahn, M. *Macromol. Rapid Commun.* **2004**, *25*, 1615. (d) Chuang, V. P.; Gwyther, J.; Mickiewicz, R. A.; Manners, I.; Ross, C. A. *Nano Lett.* **2009**, *9*, 4364. (e) Wurm, F.; Hilf, S.; Frey, H. *Chem.—Eur. J.* **2009**, *15*, 9068. (f) Yufa, N.; Fronk, S.; Darling, S. B.; Divan, R.; Lopes, W.; Sibener, S. J. *Soft Matter* **2009**, *5*, 1683.

(10) (a) Cheng, J. Y.; Ross, C. A.; Chan, V. Z. H.; Thomas, E. L.; Lammertink, R. G. H.; Vancso, G. J. *Adv. Mater.* **2001**, *13*, 1174. (b) Lu, J.; Chamberlin, D.; Rider, D. A.; Liu, M.; Manners, I.; Russell, T. P. *Nanotechnology* **2006**, *17*, 5792.

(11) (a) Lastella, S.; Jung, Y. J.; Yang, H.; Vajtai, R.; Ajayan, P. M.; Ryu, C., Y.; Rider, D. A.; Manners, I. *J. Mater. Chem.* **2004**, *14*, 1791. (b) Hinderling, C.; Keles, Y.; Stöckli, T.; Knapp, H. F.; Arcos, T. d. l.; Oelhafen, P.; Korczagin, I.; Hempenius, M. A.; Vancso, G. J.; Pugin, R.; Heinzelmann, H. *Adv. Mater.* **2004**, *16*, 876. (c) Lu, J. Q.; Kopley, T. E.; Moll, N.; Roitman, D.; Chamberlin, D.; Fu, Q.; Liu, J.; Russell, T. P.; Rider, D. A.; Manners, I.; Winnik, M. A. *Chem. Mater.* **2005**, *17*, 2227. (d) Rider, D. A.; Liu, K.; Eloi, J.-C.; Vanderark, L.; Yang, L.; Wang, J.-Y.; Grozea, D.; Lu, Z.-H.; Russell, T. P.; Manners, I. *ACS Nano* **2008**, *2*, 263. (e) Lastella, S.; Mallick, G.; Woo, R.; Karna, S. P.; Rider, D. A.; Manners, I.; Jung, Y. J.; Ryu, C., Y.; Ajayan, P. M. *J. Appl. Phys.* **2006**, *99*, 024302.

(12) (a) Massey, J. A.; Temple, K.; Cao, L.; Rharbi, Y.; Raez, J.; Winnik, M. A.; Manners, I. *J. Am. Chem. Soc.* **2000**, *122*, 11577. (b) Cao, L.; Manners, I.; Winnik, M. A. *Macromolecules* **2002**, *35*, 8258.

(13) Wang, X.; Guerin, G.; Wang, H.; Wang, Y.; Manners, I.; Winnik, M. A. *Science* **2007**, *317*, 644.

(14) (a) Loo, Y.-L.; Register, R. A.; Ryan, A. J.; Dee, G. T. *Macromolecules* **2001**, *34*, 8968. (b) Hsiao, M.-S.; Zheng, J. X.; Leng, S.; Van Horn, R. M.; Quirk, R. P.; Thomas, E. L.; Chen, H.-L.; Hsiao, B. S.; Rong, L.; Lotz, B.; Cheng, S. Z. D. *Macromolecules* **2008**, *41*, 8114. (c) Zhu, D.-S.; Liu, Y.-X.; Chen, E.-Q.; Li, M.; Chen, C.; Sun, Y.-H.; Shi, A.-C.; Van Horn, R. M.; Cheng, S. Z. D. *Macromolecules* **2007**, *40*, 1570.

(15) Gilroy, J. B.; Gädt, T.; Whittell, G. R.; Chabanne, L.; Mitchels, J. A.; Richardson, R. M.; Winnik, M. A.; Manners, I. *Nature Chem.* **2010**, *2*, 566.

(16) Gädt, T.; Ieong, N. S.; Cambridge, G.; Winnik, M. A.; Manners, I. *Nature Mater.* **2009**, *8*, 144.

(17) (a) Wang, H.; Lin, W.; Fritz, K. P.; Scholes, G. D.; Winnik, M. A.; Manners, I. *J. Am. Chem. Soc.* **2007**, *129*, 12924. (b) Wang, H.; Patil, A. J.; Liu, K.; Petrov, S.; Mann, S.; Winnik, M. A.; Manners, I. *Adv. Mater.* **2009**, *21*, 1805.

(18) (a) Portinha, D.; Boue, F.; Bouteiller, L.; Carrot, G.; Chassenieux, C.; Pensec, S.; Reiter, G. *Macromolecules* **2007**, *40*, 4037. (b) Xu, J.-T.; Fairclough, J. P. A.; Mai, S.-M.; Ryan, A. J. *J. Mater. Chem.* **2003**, *13*, 2740. (c) Chen, C.-K.; Lin, S.-C.; Ho, R.-M.; Chiang, Y.-W.; Lotz, B. *Macromolecules* **2010**, *43*, 7752. (d) Mihut, A. M.; Chiche, A.; Drechsler, M.; Schmalz, H.; Di Cola, E.; Krausch, G.; Ballauff, M. *Soft Matter* **2009**, *5*, 208. (e) Mihut, A. M.; Drechsler, M.; Möller, M.; Ballauff, M. *Macromol. Rapid Commun.* **2010**, *31*, 449. (f) Lazzari, M.; Scalarone, D.; Vazquez-Vazquez, C.; López-Quintela, M. A. *Macromol. Rapid Commun.* **2008**, *29*, 352. (g) Du, Z.-X.; Xu, J.-T.; Fan, Z.-Q. *Macromolecules* **2007**, *40*, 7633. (h) Du, Z.-X.; Xu, J.-T.; Fan, Z.-Q. *Macromol. Rapid Commun.* **2008**, *29*, 467. (i) Schmalz, H.; Schmelz, J.; Drechsler, M.; Yuan, J.; Walther, A.; Schweimer, K.; Mihut, A. M. *Macromolecules* **2008**, *41*, 3235. (j) Petzetakis, N.; Dove, A. P.; O'Reilly, R. K. *Chem. Sci.* **2011**, *2*, 955.

(19) (a) Manners, I. *Adv. Mater.* **1994**, *6*, 68. (b) Papkov, V. S.; Gerasimov, M. V.; Dubovik, I. I.; Sharma, S.; Dementiev, V. V.; Pannell, K. H. *Macromolecules* **2000**, *33*, 7107.

(20) Foucher, D. A.; Ziembinski, R.; Tang, B. Z.; Macdonald, P. M.; Massey, J.; Jaeger, C. R.; Vancso, G. J.; Manners, I. *Macromolecules* **1993**, *26*, 2878.

(21) Ni, Y.; Rulkens, R.; Manners, I. *J. Am. Chem. Soc.* **1996**, *118*, 4102.

(22) Flory, P. J.; Fox, T. G. *J. Polym. Sci.* **1950**, *5*, 745.

(23) Lammertink, R. G. H.; Hempenius, M. A.; Manners, I.; Vancso, G. J. *Macromolecules* **1998**, *31*, 795.

(24) Sperling, L. H. Introduction to Physical Polymer Science; 4th Ed., Wiley-Interscience, 2006.

(25) Lammertink, R. G. H.; Hempenius, M. A.; Vancso, G. J. *Macromol. Chem. Phys.* **1998**, *199*, 2141.

(26) Strobl, G. *Prog. Polym. Sci.* **2006**, *31*, 398.

(27) Marand, H.; Xu, J.; Srinivas, S. *Macromolecules* **1998**, *31*, 8219.

(28) (a) Henschke, O.; Knorr, J.; Arnold, M. *J. Macromol. Sci., Part A* **1998**, *35*, 473.(b) It should be noted that a recent SAXS study by Rehahn and co-workers (ref 29) estimates the equilibrium melting point of PFDMS to be 215 °C, which is significantly higher than the equilibrium melting point of PFDMS determined by the Hoffman−Weeks equation (145 °C). The same study also showed that the Hoffman−Weeks plots for PFDMS samples deviate from linearity at high crystallization temperatures. It is likely that similar effects may operate for PFDES. (c) In addition, it should also be noted that the assignment of the first rather weak endothermic transition in the heating scans of the PFDES samples to the first melting process of thin lamellae is not completely unambiguous since it could also arise due to a superposition of melting and recrystallization processes.

(29) Xu, J.; Bellas, V.; Jungnickel, B.; Stühn, B.; Rehahn, M. *Macromol. Chem. Phys.* **2010**, *211*, 1261.

(30) Rasburn, J.; Petersen, R.; Jahr, R.; Rulkens, R.; Manners, I.; Vancso, G. J. *Chem. Mater.* **1995**, *7*, 871.

(31) (a) Wang, H.; Winnik, M. A.; Manners, I. *Macromolecules* **2007**, *40*, 3784. (b) Wang, X.; Liu, K.; Arsenault, A. C.; Rider, D. A.; Ozin, G. A.; Winnik, M. A.; Manners, I. *J. Am. Chem. Soc.* **2007**, *129*, 5630.

(32) Guerin, G.; Wang, H.; Manners, I.; Winnik, M. A. *J. Am. Chem. Soc.* **2008**, *130*, 14763.

(33) Raez, J.; Manners, I.; Winnik, M. A. *Langmuir* **2002**, *18*, 7229.

(34) Bean, J. C. *Science* **1985**, *230*, 127.